

# COMBINED USE OF PARALLEL PLATE COMPRESSION AND FINITE ELEMENT MODELLING TO ANALYSE MECHANICAL PROPERTIES OF INTACT PORCINE LENS

Kehao Wang\*

*School of Science and Technology, Nottingham Trent University  
Clifton campus, Clifton Lane, Nottingham, NG11 8NS, UK  
kehao.wang@ntu.ac.uk*

Demetrios T. Venetsanos

*School of Mechanical, Aerospace and Automotive Engineering,  
Coventry University, Priory Street, Coventry, CV1 5FB, UK  
ac6109@coventry.ac.uk*

Jian Wang

*Faculty of Science Engineering and Computing, Kingston University  
Penrhyn Road, Kingston-upon-Thames, KT1 2EE, UK  
j.wang@kingston.ac.uk*

Barbara K. Pierscionek

*School of Science and Technology, Nottingham Trent University  
Clifton campus, Clifton Lane, Nottingham, NG11 8NS, UK  
barbara.pierscionek@ntu.ac.uk*

The objective of this study is to explore the feasibility of a compression test for measuring mechanical properties of intact eye lenses using novel parallel plate compression equipment to compare the accuracy of implementing a classical Hertzian model and a newly proposed adjusted Hertzian model to calculate Young's modulus from compression test results using Finite Element Analysis. Parallel-plate compression tests were performed on porcine lenses. An axisymmetric Finite Element model was developed to simulate the experimental process to evaluate the accuracy of using the classical Hertzian theory of contact mechanics as well as a newly proposed adjusted Hertzian theory model for calculating the equivalent Young's modulus. By fitting the force-displacement relation obtained from Finite Element simulations to both the classical and adjusted Hertzian theory model and comparing the calculated modulus to the input modulus of the Finite Element model, the results demonstrated that the classical Hertzian theory model overestimated the Young's modulus with a proportional error of over 10%. The adjusted Hertzian theory model produced results that are closer to original input values with error ratios all lower than 1.29%. Measurements of three porcine lenses from the parallel plate compression experiments were analysed with resulting values of Young's modulus of between 3.2 – 4.3kPa calculated. This study demonstrates that the adjusted Hertzian theory of contact mechanics can be applied in conjunction with the parallel-plate compression system to investigate the overall mechanical behaviour of intact lenses. **Keywords:** Biomechanical behaviors; intact porcine lens; parallel-plate compression; Finite element modelling (FEM); Hertzian model; Young's modulus.

## 1. Introduction

The ability of the eye to accommodate is known to decrease with age and this decrease has been well documented and characterised. However, understanding of the mechanism of accommodation and the process of presbyopia requires further investigation and is partially hampered by a paucity of knowledge about the material properties of the lens and how these alter with age. One of the difficulties in obtaining such information is in the diversity of proposed measuring techniques and the importance of conducting these on intact lenses and minimising any changes in biological properties or hydration levels during measurement. The variations in protein density across the lens and the superimposed changes with age<sup>1</sup> render any measurement of a whole lens a spatial and temporal approximation. Localised measurements require slicing or cutting which alter tissue properties and risk introducing inaccuracies in the results. Scarcity of human tissue and in particular from healthy, young donors necessitates the use of animal lenses, most frequently porcine, as these are deemed to be sufficiently physiologically representative of the human lens<sup>2</sup> and to have a similar shear elastic modulus as young human lenses<sup>3</sup>.

\*Corresponding author

An early compression study using a mechano-electric transducer to determine lens elasticity<sup>4</sup> and a subsequent, more recent, study adopting a pressure transducer<sup>5</sup> on human lenses as well as those applying compression to mouse lenses<sup>6-8</sup> all reported the general resistance of the lens to external deformation; the resistance was shown to increase logarithmically with age<sup>5</sup>. Many recent studies were able to quantify the spatially varying elasticities of lenses using various measuring techniques, ie indentation<sup>9</sup>, bubble acoustics<sup>10</sup>, and Brillouin light scattering analysis<sup>11</sup>. Results from these studies are helpful as they suggested possible relations between biomechanical properties and spatially varying protein densities of lenses and pioneered the directions for future research. Nevertheless, understanding the mechanical performance of an overall lens is of equal significance as the lens fibres and capsule behave as an integral element during accommodation. Knowing the mechanical changes of both the overall lens and of each of its constituent components with age will allow a qualitative assessment of the contribution played by different components to the decreasing accommodative ability of a whole lens with age.

This study utilizes a parallel-plate compression configuration to measure the overall elasticity of porcine lenses, and to demonstrate the feasibility of compression test for measuring the mechanical properties of the intact lens. An axisymmetric Finite Element model was developed to evaluate differing analytical method used for the calculation of the lens equivalent elastic modulus: the classical Hertzian theory model<sup>12-13</sup> and a newly proposed adjusted Hertzian theory model<sup>14</sup>. The adjusted Hertzian theory model included an adjustment ratio to include consideration of the large deformation effect of soft materials during compression.

## 2. Materials and Methods

### 2.1 Experimental procedure

The Porcine eyeballs from 6-month old animals were provided from local abattoirs and used within 8 hours of death. Lenses were removed from eyeballs keeping capsules intact and placed in a fluid bath of physiologically-balanced buffer for measurement. No ethical approval was required as the tissue was obtained from animals culled for other purposes. Measurements were conducted using a parallel plate compression configuration (MicroSquisher, CellScale) with the schematic representation shown in Fig. 1A. Deformation was applied by the microbeam, fixed to the vertical stage and controlled by the actuator, through a stainless-steel plate rigidly glued to the flexible end. The compression force was calculated by the integrated software (SquisherJoy, ver. 5.23, Waterloo, Ontario, Canada) by measuring the deflection of the microbeam in response to the pre-defined displacements. The tip displacement captured by the imaging system provided the lens deformation. The fluid bath was heated by a resistance foil heater from the base to maintain room temperature<sup>5, 11</sup> of  $26.9^{\circ} \pm 0.1^{\circ}\text{C}$ .

Representative images captured by the imaging system for a porcine lens are shown with the stainless-steel plate just above the lens (Fig. 1B), in contact with the lens (Fig. 1C) and compressing the lens (Fig. 1D). Measurements were conducted on three porcine lenses. There was no slippage of the lens samples observed and plates were carefully centred on the poles by viewing the sample on the computer at a magnification of 82x. A sinusoidal oscillatory deformation at a frequency of 0.014Hz was applied to each lens. The amplitudes of displacement and the output force and their phase difference were determined to calculate the damping ratio of each case<sup>3</sup>.

Lens sagittal widths and equatorial diameters for porcine lenses were measured using calipers and a millimetre scale and compared before and after the experiments, and these were conducted on both anterior and posterior surfaces and therefore for a longer duration, to check whether the testing produced any swelling or shrinkage of the lenses. Porcine lenses had a mean equatorial diameter of 13.5mm and a mean sagittal width of 11mm. No identifiable swelling or shrinkage was found after experimentation.

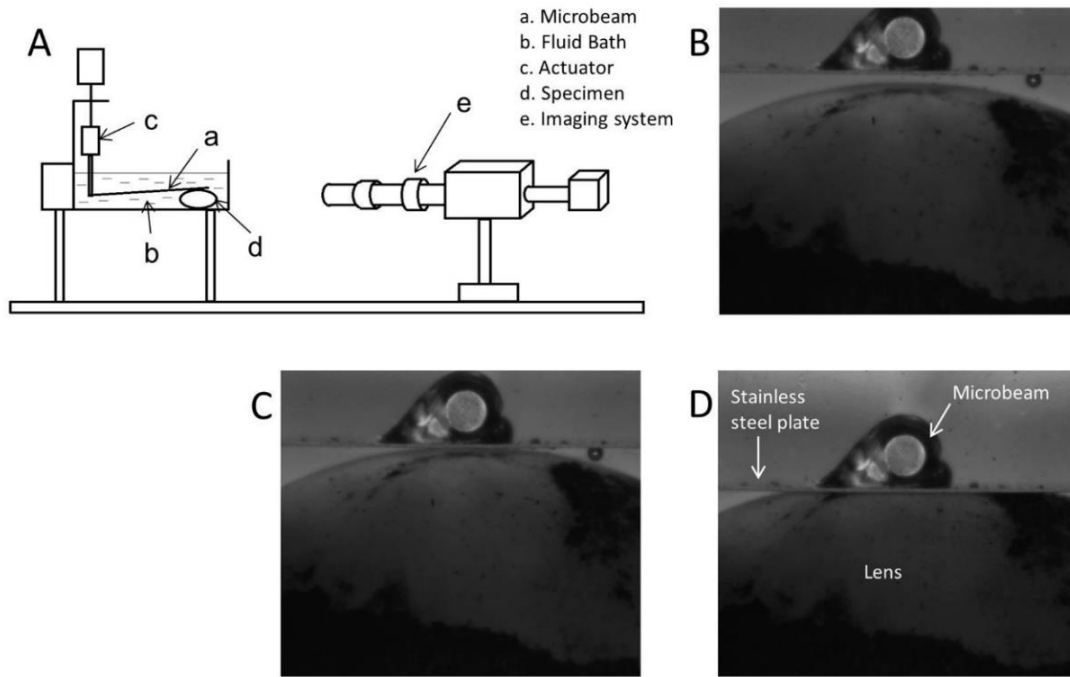


Fig. 1. A— Schematic representation of the testing configuration, recorded images of an intact porcine lens when the stainless steel plate; B— is just above the lens; C— in contact with the lens and D— compressing the lens.

## 2.2 FEM based feasibility analysis of analytical models

The study of deformation between two bodies in touch with each other at single or multiple points is within the scope of contact mechanics<sup>13</sup>. The classical contact theory of Hertz solves the problem of two elastic bodies with curved surfaces coming into contact with a resulting small deformation induced by the applied force. The amount of deformation is dependent on the both the surface curvatures and elastic moduli of the two bodies. Hertzian theory can be applied to analyse the diametric compression test in the present study by assuming one body as infinite large half space, ie, the radius of curvature being treated as infinitely large<sup>12-13</sup>.

### 2.2.1 Data analysis using classical Hertzian theory

The force-displacement relationship during elastic contact between a sphere and a single flat plate is given by equation (1):<sup>12</sup>

$$F = \frac{4}{3(1-\nu^2)} E \sqrt{R} d^{3/2} \quad (1)$$

where  $d$  is the displacement of the flat plate,  $R$  is the radius of curvature of the sphere,  $\nu$  is Poisson's ratio = 0.5 and  $E$  is Young's modulus.

The lens in the present diametric test was deformed on both sides, where it was in contact with the base of the fluid bath as well as the stainless steel plate and was assumed to be deformed symmetrically on both sides, giving the recorded displacement of the stainless-steel plate relative to the base of the fluid bath  $\delta$  equal to  $2d$ . Rearranging equation (1) gives:

$$F = \frac{E \sqrt{2R} \delta^{3/2}}{3(1-\nu^2)} \quad (2)$$

The radius of curvature ( $R$ ) of the undeformed lens surface in contact with the stainless-steel plate during compression was determined within the lens central 4.4mm zone which is the maximum width of the recorded image.

Excluding Young's modulus  $E$ , the rest terms in equation (2) can be collectively represented as  $X$ :

$$X = \frac{\sqrt{2R}\delta^{3/2}}{3(1-\nu^2)} \quad (3)$$

The force  $F$  is linearly related to the term  $X$  by Young's modulus  $E$ , a constant ratio describing the elastic properties of the intact lens, as described in equation (4):

$$F = EX \quad (4)$$

Fig. 2a shows the linear relationship between force  $F$  and the term  $X$  for an intact porcine lens, where Young's modulus  $E$  is seen as the slope of the linear regression line.

### 2.2.2 Data analysis using adjusted Hertzian theory

An assumption of using Hertzian contact theory is that the strain is small and within the elastic limit. As pointed out by Ding et al.<sup>14</sup>, biological tissues and cells subjected to compression testing usually undergo large deformation. Ding et al.<sup>14</sup> proposed an adjusted Hertzian model by adding an adjustment parameter,  $\alpha$ , into the force-displacement relationship:

$$F = \frac{4}{3(1-\nu^2)} E\sqrt{R}d^{3/2} \left(1 + \alpha \frac{d}{R}\right) \quad (5)$$

Considering  $\delta=2d$  in the present study, equation (5) could be rewritten as:

$$F = \frac{E\sqrt{2R}\delta^{3/2}}{3(1-\nu^2)} \left(1 + \alpha \frac{\delta}{2R}\right) \quad (6)$$

The adjustment parameter  $\alpha$  is dependent on the geometry of the experimental system, ie the ratio of radius between the compressor and the sample<sup>14</sup>. The compressor in the present study was a flat disc that can be treated as having an infinitely large radius; the best-fitted value  $\alpha$  was found to be 3 based on the analysis from Ding et al.<sup>14</sup>. According to the adjusted Hertzian model, the force is linearly related to a term  $X'$  by the constant value of Young's modulus  $E$ . The term  $X'$  is described in equation (7):

$$X' = \frac{\sqrt{2R}\delta^{3/2}}{3(1-\nu^2)} \left(1 + \alpha \frac{\delta}{2R}\right) \quad (7)$$

The linear relationship between  $F$  and  $X'$  is shown in equation (8) and plotted in Fig. 2b for an intact porcine lens:

$$F = EX' \quad (8)$$

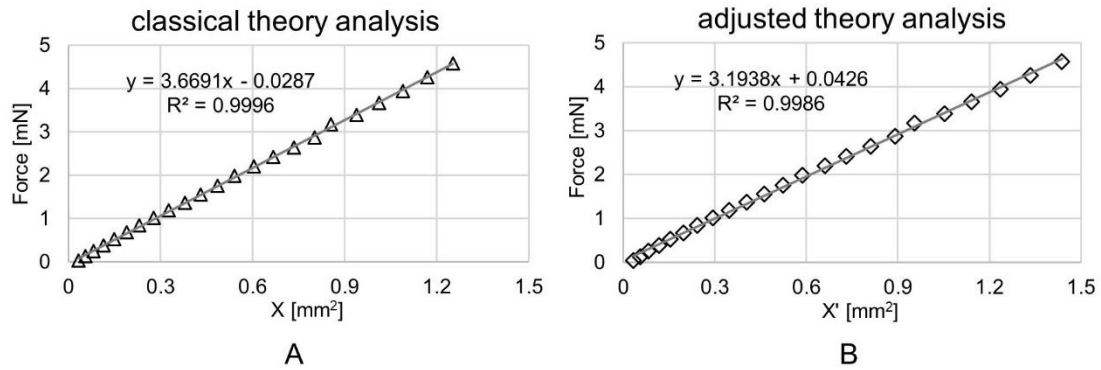


Fig.2. Analysis of Young’s moduli of an intact porcine lens with linear relationships shown between A— F and X for analysis using the classical Hertzian theory and B— F and X’ for analysis using adjusted Hertzian theory.

### 2.2.3 FEA assessment

To assess the accuracy of applying the Hertzian model in the data analysis of the current compression study, a Finite Element (FE) porcine lens model was developed to simulate the same situation as that of the experimental process. The geometry of the porcine lens model (demonstrated in Fig. 3a) was constructed from Hahn et al.<sup>15</sup> by fitting a spline curve in SolidWorks (ver. 2017, Waltham, Massachusetts, USA) to the undeformed porcine lens shape before laser surgery shown in Fig. 9 of Hahn et al.<sup>15</sup>. The detailed shape parameters defining the spline curve are listed in Table 1. An axisymmetric FE model as shown in Fig. 3b was developed in Ansys Mechanical APDL (ver. 18.2, Canonsburg, Pennsylvania, USA). All parts of the model were meshed with 8-node axisymmetric plane element (ANSYS element type: PLANE183). The two compressing plates were modelled as rigid bodies. The porcine lens was simulated with six different overall Young’s moduli selected within the range reported in the literature<sup>16-17</sup>. A Poisson’s ratio of 0.49 was used under the consideration of the nearly incompressible character of porcine lenses. A compression force of 4.5mN, at a similar magnitude of the value employed by the indentation test of Heys et al.<sup>9</sup>, was applied perpendicular to the upper rigid plate in 30 steps. Nonlinear geometrical analysis was performed as described previously<sup>18-19</sup>.

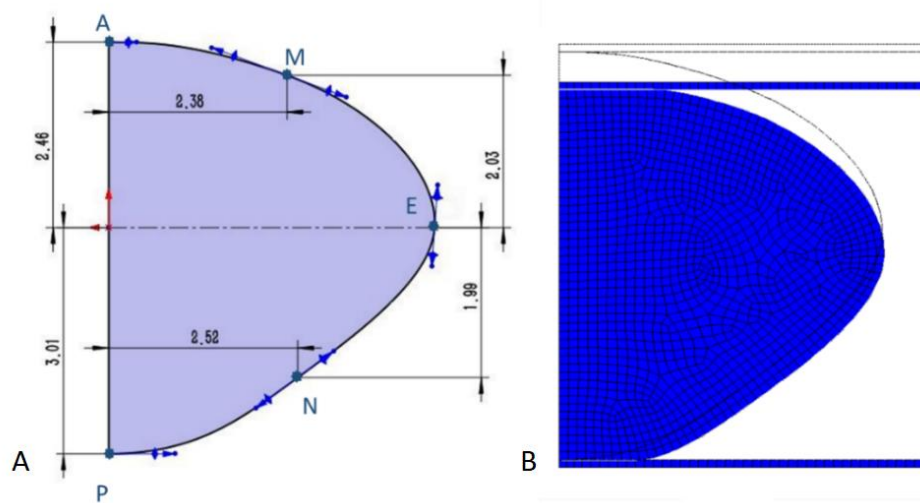


Fig.3. A— Geometry of a porcine lens shape taken from Hahn et al.<sup>15</sup> and B— deformed FE porcine lens model of the porcine lens being compressed by a rigid plate.

Table 1. Shape parameters of the porcine lens model reanalysed from Hahn et al.<sup>15</sup>

point	x coordinate (mm)	y coordinate (mm)	Tangent weighting 1	Tangent weighting 2	Tangent radial direction (degree)
A	0	2.46	0	1.57	180.00
P	0	-3.01	3.67	0	0.00
E	4.35	0	2.38	2.18	-85.87
M	2.38	2.03	3.85	3.47	-159.82
N	2.52	-1.99	2.53	2.66	-36.10

The relation between the compression force and the resultant displacements of the upper plate in the vertical direction was analysed for each simulated Young's modulus. Theoretical calculations were repeated for these force-displacement relationships obtained from FE simulations using the same procedure as described in section 2.2.1 for classical Hertzian analysis and in section 2.2.2 for the adjusted Hertzian analysis. The calculated Young's modulus was compared with the input Young's modulus of the FE model for determination of the error ratio (listed in Table 2).

### 3. Results

For six simulated Young's moduli that were input parameters to the FE model, the resultant changes in vertical displacements of the upper rigid plate in response to the applied compression force assessed with both classical Hertzian theory, using Equation (4), and the adjusted Hertzian theory, using Equation (8), are listed in Table 2. Using the classical Hertzian model, the calculated Young's moduli were higher than the actual values introduced into the FE model for each simulated case and the proportional errors were all higher than 10%. Young's moduli calculated with the adjusted Hertzian model were closer to the input values; the error ratios were all lower than 1.29%.

Table 2. Young's moduli simulated with the FE model and the calculated values using the Hertzian as well as the corrected Hertzian model.

Input modulus (kPa)	1.0000	2.0000	3.0000	4.0000	5.0000	6.0000
Calculated with classical Hertzian theory (kPa)	1.1381	2.2853	3.3832	4.4689	5.6091	6.6986
Error ratio	0.1381	0.1427	0.1277	0.1172	0.1218	0.1165
Calculated with adjusted Hertzian model (kPa)	0.9961	2.0257	3.0177	3.9979	5.0162	6.0004
Error ratio	0.0039	0.0129	0.0059	0.0005	0.0032	0.0001

Young's moduli of porcine lenses measured with both classical Hertzian model and adjusted Hertzian model were listed in Table 3. Compared with the adjusted Hertzian model, the classical Hertzian model generally estimated a higher Young's modulus of each lens. Young's modulus resulted from the present study, ranges from 3.2kPa to 5.2kPa, are within the range of 0.6kPa to 5.7kPa obtained from previous studies<sup>16-17</sup>. The damping ratios of each porcine lens was found to be much smaller than 1.

Table 3. Radius of curvature and Young's modulus (E) of the tested intact lenses

	Porcine lens 1	Porcine lens 2	Porcine lens 3
Radius of curvature	8mm	7mm	8mm
Damping ratio	0.054	0.097	0.028
E (classical Hertzian model)	3.7 kPa	5.2 kPa	4.9 kPa
E (adjusted Hertzian model)	3.2 kPa	4.3 kPa	4.1 kPa

Additionally, all measured lenses demonstrated a hysteresis effect; the loading and unloading paths of the force and displacement curves form hysteresis loops (as shown in Fig. 4). Porcine lens 2 demonstrated a much higher hysteresis effect than the other two porcine lenses.

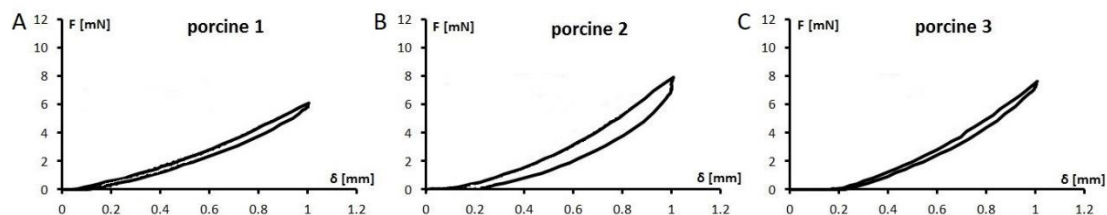


Fig.4. Hysteresis curve of measured intact porcine lenses.

#### 4. Discussion

Various types of measuring techniques have been developed for determining the mechanical properties of the lens. These techniques and the parameters they seek to measure vary widely. Newly advanced methods including indentation<sup>9</sup>, bubble acoustics<sup>2,10</sup> and Brillouin scattering<sup>20</sup> have investigated localized variations in lens biomechanical properties. Some studies have employed dynamic measurements using a rheometer and determined lens viscoelastic behaviour over a range of measured frequencies<sup>3,21</sup>. Indentation studies were performed on equatorial planes of sectioned lenses that had been frozen and thawed and disturbances to the lens fibre alignment by sectioning can result in dehydration<sup>22</sup>. Bubble-acoustic methods rely on the measurement of displacement and size of a bubble induced by an ultrafast laser<sup>2</sup>; the modulation of lens local densities induced by the laser cannot be neglected.

Non-invasive methods such as spinning<sup>23-24</sup> and compression<sup>4-5</sup> determine the overall mechanical properties of the lens with the advantage of maintaining the lens intact. Spinning applies centrifugal forces causing the lens to assume a flatter shape and the overall elastic modulus of the lens is determined from the changing shape parameters of the spinning lens<sup>23-24</sup>. Brillouin scattering, uniquely, has the potential to be performed *in vivo* but is currently limited to characterizing only the compressional modulus because of the frequency applied<sup>25-26</sup>.

The present study evaluated the accuracy of applying Hertzian contact theory<sup>12-13</sup> for analysing data collected in diametric compression testing using FE models. It was recently demonstrated by Ding et al.<sup>14</sup> that the classical Hertzian theory model needs to include an adjustment ratio to be used for measuring biological tissues and soft materials. The adjusted model proposed by Ding et al.<sup>14</sup> was based on an atomic force microscopic measuring system in which the compressor has a spherical shape. According to the analysis by Ding et al.<sup>14</sup>, the adjustment ratio  $\alpha$  is dependent on the ratio of the radius between the compressor and the sample. In the present study, the compressor as a flat plate can be treated as having an infinitely large radius, which results in a constant value of  $\alpha = 3$  regardless of the sample radius. The Hertzian theory was previously applied on gel phantoms with a lens geometry<sup>27</sup> but has never been applied to real lenses. The capsule was kept intact during the compression so as to prevent any water loss and dehydration; hence, the resulting elastic moduli include the contribution of capsular elasticity and serve as equivalent Young's moduli of the whole lens system. In a bubble-acoustic study<sup>16</sup>, the gradient moduli in four porcine lenses gave values of elastic moduli from 1.2kPa to 5.7kPa; Young's moduli of porcine lenses measured in this study are comparable, varying from 3.2kPa to 4.1kPa. In a

spinning study of porcine lenses<sup>17</sup>, the spatially varying shear modulus ranged from 0.2 to 0.7 kPa. Shear modulus  $G$  is converted into Young's modulus using  $E=3G$  (treating the lens as incompressible, ie Poisson's ratio = 0.5). The converted Young's moduli reported by the spinning test are found to be in the range of 0.6kPa to 2.1kPa, slightly lower than that reported by the present study albeit with individual variations. Assumptions made when applying Hertzian analysis were that the material properties were homogeneous for the lens and capsule as a single system; and that there were no adhesions between the bottom of the tank and the lens samples.

All lenses demonstrated hysteretic behaviour. The tested frequency in the present study was 0.014Hz and the damping ratios of all the tested lenses under such low frequencies were  $\ll 1$ , which indicate that the lenses were underdamped. Weeber et al.<sup>28</sup> investigated human lenses over the frequency range from 0.001 to 30Hz and found that both elastic behaviour and viscous behaviour are dependent upon frequency. Viscous effects and the hysteresis loop were more pronounced when a higher frequency rather than a lower one was applied<sup>29</sup>. Schachar et al.<sup>3</sup> reported that porcine lenses are overdamped and are more viscous than elastic over the frequency ranges tested: 10-50Hz; human lenses also have higher viscous than elastic shear moduli at three frequencies: 50, 75 and 150Hz<sup>21</sup>. The mechanical properties of lenses are dependent on the time scale of observation: slow deformation of the tissue occurs elastically but rapid deformation is strongly resisted because of viscous properties; viscosity will give a greater resistance at higher frequencies<sup>30</sup>. The frequency used in the present study was in the lower limit of those dynamic tests and for this range of frequencies elastic behaviour predominated over viscous behaviour. The interaction of lens fibre membrane and the cytoskeleton forming the elastic portion as well as the intra and intercellular fluids representing the viscous portion, is thought to contribute to the viscoelastic behaviour of the lens<sup>3,21</sup>. The existence of reliable approaches for investigating this viscoelastic nature of the lens may provide a better understanding of presbyopia and potentially aid in the design of new generation accommodating implant lenses. Measurement of lens material properties will provide different results depending on what is being sought and the method used: compression<sup>4-5</sup>, oscillatory indentation<sup>31</sup> and rheometry<sup>3,21</sup> are capable of measuring dynamic mechanical response, while methods like bubble-acoustics<sup>2,10</sup> and Brillouin scattering analysis<sup>25-26</sup> are applicable for static measures. Notably, the state - *in vivo* or *in vitro*, post-mortem time, frozen and thawed or fresh sample as well as age of the lens - will provide the greatest variations in findings. Future studies on more and higher frequencies are needed for a comprehensive understanding of lens mechanical properties.

It is vital to examine both the spatially varying material properties of lenses as well as their overall resistance because the latter describes the general *in vivo* lens behaviour. A number of studies have investigated the spatially varying material properties of the lens<sup>19,20,31</sup> gradient elastic moduli were found<sup>20,32</sup>. The compression test reported in the present study adds to the body of literature and is appropriate for quantifying the overall intact lens performance which is relevant to the physiological condition.

## 5. Conclusions

The accuracy of applying the classical and an adjusted Hertzian theory model to determine the mechanical properties of intact porcine lenses was evaluated with the utilization of Finite Element models. The adjusted Hertzian theory model provided closer estimations of Young's modulus to the original input values than the classical Hertzian model. The parallel-plate compression system can be used to investigate the mechanical behaviour of intact lenses when combined with the adjusted Hertzian theory model, as the provided Young's moduli of porcine lenses are similar to those obtained from the literature. Further analyses using higher frequencies should be applied to biological samples to characterize more fully the viscoelastic properties of lenses.

## References



1. Pierscionek BK, Regini JW, The gradient index lens of the eye: an opto-biological synchrony, *Prog Retin Eye Res* **31**: 332-349, 2012.
2. Erpelding TN, Hollman KW, O'Donnell M, Mapping age-related elasticity changes in porcine lenses using bubble-based acoustic radiation force, *Exp Eye Res* **84**: 332-341, 2007.
3. Schachar RA, Chan RW, Fu M, Viscoelastic shear properties of the fresh porcine lens, *Br J Ophthalmol* **91**: 366-368, 2007.
4. Kikkawa Y, Sato T, Elastic properties of the lens, *Exp Eye Res* **2**: 210-215, 1963.
5. Glasser A, Campbell MC, Biometric, optical and physical changes in the isolated human crystalline lens with age in relation to presbyopia, *Vision Res* **39**: 1991-2015, 1999.
6. Gokhin DS, Nowak RB, Kim NE, Arnett EE, Chen AC, Sah RL, Clark JI, Fowler VM, Tmod1 and CP49 synergize to control the fiber cell geometry, transparency, and mechanical stiffness of the mouse lens, *PLoS One* **7**: e48734, 2012.
7. Fudge DS, McCuaig JV, Van Stralen S, Hess JF, Wang H, Mathias RT, FitzGerald PG, Intermediate filaments regulate tissue size and stiffness in the murine lens, *IOVS* **52**: 3860-7, 2011.
8. Baradia H, Nikahd N, Glasser A, Mouse lens stiffness measurements, *Exp Eye Res* **91**: 300-7, 2010.
9. Heys KR, Cram SL, Truscott RJ, Massive increase in the stiffness of the human lens nucleus with age: the basis for presbyopia? *Mol Vis* **10**: 956-963, 2004.
10. Hollman KW, O'Donnell M, Erpelding TN, Mapping elasticity in human lenses using bubble-based acoustic radiation force, *Exp Eye Res* **85**: 890-893, 2007.
11. Besner S, Scarcelli G, Pineda R, Yun S, In vivo Brillouin analysis of the aging human lens, *Invest. Ophthalmol. Vis. Sci* **57**: 5093-5100, 2016.
12. Portnikov D, Kalman H, Determination of elastic properties of particles using single particle compression test *Powder Technol* **268**: 244-252, 2014.
13. Johnson KL, Contact mechanics *Cambridge university press*, 1987.
14. Ding R, Xu G, Wang G, On the determination of elastic moduli of cells by AFM based indentation, *Sci. Rep* **7** 45575, 2017.
15. Hahn J, Fromm M, Halabi FA, Besdo S, Lubatschowski H, Ripken T, Kruger A, Measurement of Ex Vivo porcine lens shape during simulated accommodation, before and after fs-Laser treatment, *IOVS* **56**: 5332-5343, 2015.
16. Yoon S, Aglyamov S, Karpiouk A, Emelianov S, The mechanical properties of ex vivo bovine and porcine crystalline lenses: age-related changes and location-dependent variations *Ultrasound Med Biol* **39**: 1120-1127, 2013.
17. Reilly MA, Martius P, Kumar S, Burd HJ, Stachs O, The mechanical response of the porcine lens to a spinning test *Zeitschrift für Medizinische Physik* **26**: 127-135, 2016.
18. Burd HJ, Judge SJ, Flavell M J, Mechanics of accommodation of the human eye, *Vision Research* **39**: 1591-1595, 1999.
19. Wang K, Venetsanos D, Wang J, Pierscionek BK, Gradient moduli lens models: how material properties and application of forces can affect deformation and distributions of stress *Sci Rep* **6**, 2016. DOI: 10.1038/srep31171
20. Scarcelli G, Kim P, Yun SH, In vivo measurement of age-related stiffening in the crystalline lens by Brillouin optical microscopy *Biophys J* **101**: 1539-1545, 2011.
21. Schachar RA, Chan RW, Fu M, Viscoelastic properties of fresh human lenses under 40 years of age: implications for the aetiology of presbyopia, *Br J Ophthalmol* **95**: 1010-1013, 2011.
22. Lahm D, Lee LK, Bettelheim FA, Age dependence of freezable and nonfreezable water content of normal human lenses, *Invest. Ophthalmol. Vis. Sci* **26**: 1162-1165, 1985.
23. Fisher R, The elastic constants of the human lens, *J Physiol (Lond.)* **212**: 147-180, 1971.
24. Wilde G, Burd H, Judge S, Shear modulus data for the human lens determined from a spinning lens test, *Exp Eye Res* **97**: 36-48, 2012.
25. Bailey ST, Twa MD, Gump JC, Venkiteshwar M, Bullimore M, Sooryakumar R, Light-scattering study of the normal human eye lens: elastic properties and age dependence, *Biomedical Engineering, IEEE Trans Biomed Eng* **57**: 2910-2917, 2010.
26. Reiß S, Burau G, Stachs O, Guthoff R, Stolz H, Spatially resolved Brillouin spectroscopy to determine the rheological properties of the eye lens, *Biomed opt Express* **2**: 2144-2159, 2011.
27. Ravi N, Wan KT, Swindle K, Hamilton PD, Duan G, Development of techniques to compare mechanical properties of reversible hydrogels with spherical, square columnar and ocular lens geometry, *Polymer* **47**: 4203-9, 2006.
28. Weeber HA, Eckert G, Soergel F, Meyer CH, Pechhold W, van der Heijde RG, Dynamic mechanical properties of human lenses, *Exp Eye Res* **80**: 425-434, 2005.
29. Hopkinson B, Williams GT, The elastic hysteresis of steel, *Proceedings of the Royal Society of London. Series A* **87**: 502-511, 1912.
30. Low JL, Reed A, Basic biomechanics explained *Butterworth-Heinemann Medical*, 1996.
31. Weeber HA, Eckert G, Pechhold W, van der Heijde, Rob GL, Stiffness gradient in the crystalline lens *Graefes Arch Clin Exp*

*K. Wang et al.*

*Ophthalmol* **245**: 1357-1366, 2007.

32. Scarcelli G, Yun SH, In vivo Brillouin optical microscopy of the human eye *Opt Express* **20**: 9197-9202, 2012.